

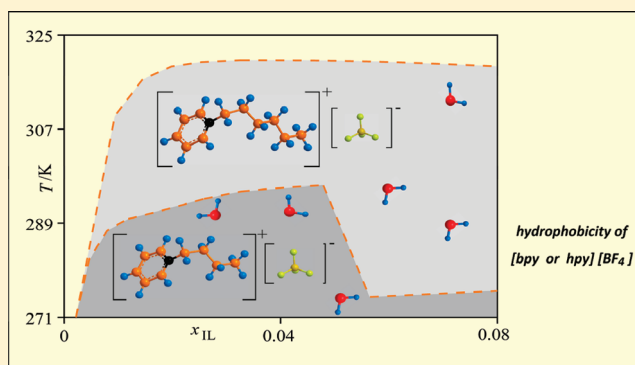
Thermodynamic Behavior of the Binaries 1-Butylpyridinium Tetrafluoroborate with Water and Alkanols: Their Interpretation Using ^1H NMR Spectroscopy and Quantum-Chemistry Calculations

Remko Vreekamp, Desire Castellano, José Palomar,[†] Juan Ortega,^{*} Fernando Espiau, Luís Fernández, and Eduvigis Penco

Laboratorio de Termodinámica y Fisicoquímica de Fluidos, Parque Científico-Tecnológico, Universidad de Las Palmas de Gran Canaria, Canary Islands, Spain

S Supporting Information

ABSTRACT: Here we present experimental data of different properties for a set of binary mixtures composed of water or alkanols (methanol to butanol) with an ionic liquid (IL), butylpyridinium tetrafluoroborate $[\text{bpy}][\text{BF}_4]$. Solubility data (x_{IL}, T) are presented for each of the mixtures, including water, which is found to have a small interval of compositions in IL, x_{IL} , with immiscibility. In each case, the upper critical solubility temperature (UCST) is determined and a correlation was observed between the UCST and the nature of the compounds in the mixtures. Miscibility curves establish the composition and temperature intervals where thermodynamic properties of the mixtures, such as enthalpies H_m^E and volumes V_m^E , can be determined. Hence, at 298.15 and 318.15 K these can only be found with the first four alkanols. All mixing properties are correlated with a suitable equation $\xi(x_{\text{IL}}, T, Y_m^E) = 0$. An analysis on the influence of the temperature in the properties is shown, likewise a comparison between the results obtained here and those of analogous mixtures, discussing the position of the $-\text{CH}_3$ group in the pyridinic ring. The ^1H NMR spectra are determined to analyze the molecular interactions present, especially those due to hydrogen bonds. Additional information about the molecular interactions and their influence on the mixing properties is obtained by quantum chemistry calculations.



INTRODUCTION

This work forms part of a broader project that studies the possibilities of using ionic liquids (ILs) derived from pyridinium for a series of engineering applications. For this purpose, mixing properties are being determined using this kind of IL and common solvents, such as water and the first alkanols, helping us to establish the degree of interaction between different kinds of compounds, complemented by a suitable and necessary modeling process. Previous studies^{1–4} have analyzed the behavior of three isomers of butyl-*X*-methylpyridinium tetrafluoroborate $[\text{bXmpy}][\text{BF}_4]$ ($X = 2, 3, 4$) in solution, with the aforementioned solvents. One of the objectives of this was to study the influence of the position of the methyl group on the IL behavior in solution. However, it is also relevant to determine the influence of the presence of the $-\text{CH}_3$ in the pyridinic ring. It was, therefore, considered interesting to carry out a theoretical–experimental study of solutions containing butylpyridinium tetrafluoroborate, $[\text{bpy}][\text{BF}_4]$. This IL has been used in some applications, such as chemical reactions,⁵ lubricants,⁶ polymeric electrolytes⁷ and sulfur extracting agent,⁸ among others.

Here, we study the binary systems $[\text{bpy}][\text{BF}_4] + \text{H}_2\text{O}$ or $+ \text{C}_u\text{H}_{2u+1}(\text{OH})$ ($u = 1–4$) by experimentally determining the

basic thermodynamic properties of both the pure compounds and the solutions, especially the excess volumes V_m^E and excess enthalpies H_m^E . The study of literature shows a growing number of works on the determination of excess properties of mixtures including ILs, which have been revealed of interest for the analysis of IL–solvent interactions.^{9–11} Thus, previous works^{12,13} reported V_m^E data for the system $[\text{bpy}][\text{BF}_4] + \text{H}_2\text{O}$ at 298.15 and 318.15 K¹² and, also, the V_m^E for the binary mixtures of $[\text{bpy}][\text{BF}_4] + \text{CH}_3(\text{OH})$ or $+ \text{C}_2\text{H}_5(\text{OH})$ at different temperatures.¹³ However, we did not find any previous H_m^E data of $[\text{bpy}][\text{BF}_4]$ mixtures in the literature. It has been stated that temperature has an important effect when working with ILs since it favors miscibility and, hence, possible molecular interactions and other aspects that define its dissolution capacity.^{1–4} More precisely, with a rise in temperature some of the properties can be measured in the entire range of compositions. Therefore, before starting the experimentation regarding excess properties, it is important to define the miscibility zones, with the temperature–composition

Received: March 26, 2011

Revised: June 4, 2011

Published: June 07, 2011

curves. Once the zones of one and two phases in liquid–liquid equilibria (LLE) has been established, the excess thermodynamic properties, such as enthalpies H_m^E and volumes V_m^E of the mixtures [bpy][BF₄] + water, + CH₃(OH), + C₂H₅(OH), + C₃H₇(OH) and + C₄H₉(OH) were determined, when possible, at 298.15 and 318.15 K temperatures. For comparison purposes, the measured H_m^E and V_m^E values of [bpy][BF₄] mixtures were related to those obtained for [bXmpy][BF₄] mixtures by our group^{1–3} and, also, to the V_m^E values of [bpy][BF₄] mixtures reported by other authors.^{12,13}

Several authors^{14,15} have shown that hydrogen bonds play an important role in the interaction between the cation or the anion and solvent molecules, which are revealed by changes in their ¹H NMR chemical shifts.¹⁶ For this work, spectroscopy experiments of ¹H NMR were also carried out to obtain more information about the molecular interactions between [bpy][BF₄] and water or alkanols.

Another aim of this series of works with ILs derived from pyridinium is contributing to the development of theoretical models for predicting their thermodynamic properties. The previous experience of our group with two methods applied in the field of chemical engineering has been enriching.^{4,17} One of these, the UNIFAC group contribution method,¹⁸ is frequently employed in this area, although at the moment it has not been extensively used in IL systems because the interaction parameters between the corresponding functional groups were not generally available,¹⁹ an issue to be addressed in future studies by our team. On the other hand, the *ab initio* COSMO-RS²⁰ methodology, which predicts thermodynamic data solely using electronic information of individual molecules in the fluid, has been demonstrated to be useful for understanding the mixing behavior of [bXmpy][BF₄] + water or alkanol systems, similar to those studied here,³ allowing the comparison and analysis of the experimental data obtained, especially the mixing enthalpies H_m^E . Hence, for this work, quantum-chemistry calculations are carried out to obtain information about the molecular interactions that affect the mixing properties, which can be used to develop computational approaches that adequately simulate the behavior of solutions in order to select an appropriate IL for a specific application.

■ EXPERIMENTAL SECTION

Apparatus and Procedures. The excess volumes V_m^E were calculated from the density values, both of pure products and of mixtures, determined with a DMA-58 Anton Paar vibrating-tube digital densimeter, with a reading error of $\pm 0.02 \text{ kg} \cdot \text{m}^{-3}$. In spite of the fact that the densimeter is equipped with its own thermostating system with a Peltier effect, the apparatus was connected to a Polyscience external circulation thermostat bath with a control of $\pm 0.02 \text{ K}$ at a constant temperature of $(T - 0.5) \text{ K}$, where T corresponds to the working temperature, 298.15 or 318.15 K. In this case, the different binary mixtures were synthetically prepared by weighing them in hermetically closed glass vials and placing them in an ultrasound bath for thirty minutes to homogenize the mixture. The errors in the molar fractions in [bpy][BF₄] were estimated to be around ± 0.0002 . For the case of the ILs, the influence of the viscosity on the density values for the apparatus described was studied, both in pure compounds and in mixtures. According to the manufacturer's recommendations (www.anton-paar.com), in the case of the DMA-58 densimeter, the instrument automatically corrects

the densities of liquids with viscosities lower than $100 \text{ mPa} \cdot \text{s}$ and the corrections recommended in other cases were also applied. For our mixtures, viscosities were lower than that in most of the concentration range, so the correction is automatic, since only slight differences of $\pm 0.00003 \text{ g} \cdot \text{cm}^{-3}$ were estimated in the zones rich in IL, $x_{\text{IL}} > 0.9$, and no significant effects were observed in the zones of intermediate concentration.

A Selecta ST-100 rotational viscosimeter, with a reproducibility of 0.2%, was used to measure the viscosity of the IL. The measuring cell of the viscosimeter, with an incorporated heat exchanger, was thermostated with the thermostatic bath described, and allowed an error in the temperature control of the viscosimeter cell of $\pm 0.05 \text{ K}$. The apparatus was previously calibrated at each temperature using a standard supplied by Brookfield Engineering Laboratories. For the alkanols and water, an AMV200 falling-ball viscosimeter was used, also thermostated with the aforementioned equipment. For the [bpy][BF₄], a dynamic viscosity value of $167.3 \text{ mPa} \cdot \text{s}$ was obtained at 298.15 K, 163.3,¹² and of $50.9 \text{ mPa} \cdot \text{s}$ at 318.15 K, 55.8,¹² which were comparable to the values we obtained, with a similar water content. For the synthetic materials prepared it was found that, in most of the range of compositions, the viscosity is far lower than this and, as mentioned previously, the density is corrected automatically.

Refractive indices of the pure compounds were measured with a Zuzi 320 Abbe refractometer, with a reading error of ± 0.0002 units in n_D , thermostated with the system described above.

The H_m^E were measured directly at the two temperatures selected for this work, 298.15 and 318.15 K, in an MS80D Calvet conduction calorimeter by Setaram, Lyon (France), calibrated electrically at each temperature by a Joule effect using an EJ3 power source of the same manufacturer, which can generate analogous thermograms to the mixing processes when different values of power are applied to a special calibration cell. In all cases, the differential assembly was employed for the calorimetric process. Data were recorded and treated with the SETSOFT commercial software supplied by Setaram, carrying out the corresponding temperature corrections, between that recorded on the computer and the one indicated for the sample, to ensure that the interior of the cell is at the real temperature T selected. This was verified using a cell with paraffin oil containing a sensor connected to an F200 AFL, with a resolution of $\pm 1 \text{ mK}$. Likewise, before the experimentation the efficacy of the calorimetric block was verified with the differential measurement of the temperature of both cells (A–B), which did not exceed $\pm 2 \text{ mK}$ in any case. The apparatus was electrically calibrated independently at each of the aforementioned temperatures, and the reproducibility of the apparatus-constant was total. The correct functioning of the apparatus was verified by making measurements for the mixtures of benzene + cyclohexane at 298.15 K and benzene + propan-1-ol at 318.15 K, comparing them, respectively, with values reported in the literature^{21,22} for each of these mixtures. In both cases, reproduction of the curves presented an uncertainty lower than 1% for the H_m^E values; the average uncertainty of the IL x_{IL} composition was estimated to be $\pm 2 \times 10^{-4}$.

The H_m^E of the mixtures studied here [bmpy][BF₄] were measured twice by using two different types of cells. The first, equipped with a cylindrical minishaker, has been described in a previous paper.¹ A set of measurements were made with another cell, but only in the composition interval $0.2 \leq x_{\text{IL}} \leq 1$ for purposes of verification, which presents slight modifications of

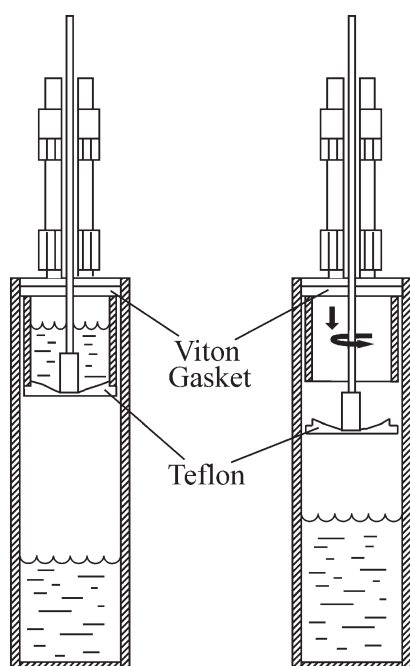


Figure 1. Scheme of experimental cell used in the mixing enthalpy measurements. Left, before mixing process; right, after mixing process.

other measurements described previously,⁴ and the scheme is shown in Figure 1. In this interval, the values obtained for H_m^E with both procedures were almost identical. The cell shown in Figure 1 is supplied optionally by Setaram to work with intermediate compositions. However, the original design has been adapted, by replacing the lower metal catch (that drops into the liquid producing strong distortions in the mixing process) by a concave Teflon catch fixed to a metal rod that protrudes out of the calorimeter. Hence, when the rod is pushed down, the IL falls from the upper minicell mixing with the liquid in the main cell, and the Teflon catch drops down to the level of the mixture. Once immersed in the liquid mixture, this can be used to briefly stir it. The thermogram produced by the experiment on a blank is subtracted from those obtained for the mixing processes of all the systems, producing net values of H_m^E .

The ^1H NMR experiments were conducted in an Avance Bruker 300 MHz spectrometer, at a temperature of 293 K, using acetone- d_6 (and D_2O) in concentric capillaries to obtain the *lock*. Chemical displacements were normalized to those of acetone- d_6 (and D_2O).

Materials. The $[\text{bpy}][\text{BF}_4]$ used in this work was supplied by IoLiTec, GmbH & Co. KG and had a commercial purity of +99 wt % and a water content <400 ppm, which was verified with a DL18 Mettler Karl Fischer volumetric analyzer, and a halide content of 87 ppm according to the manufacturer. The alkanols (methanol to butanol), of the highest commercial purity, were supplied by Aldrich and were verified using an HP6890 GC equipped with FID, to confirm the values given by the manufacturer. The $[\text{bpy}][\text{BF}_4]$ was kept and handled in a dry chamber. Before preparing the samples, all the products used in this work were degasified in an ultrasound bath for hours and the alkanols were stored over a 0.3 nm Fluka molecular sieve. The water used, both in the experiments and to calibrate the apparatus, was obtained in our laboratory by bidistillation followed by several hours degasification, and presented an electrical conductance lower than $1.5 \mu\text{S}$.

Over a broad temperature range (288–328 K), the density ρ , refraction index n_D , and dynamic viscosity η of all the substances were determined, estimating the corresponding correlation of each property M , $M = M(T)$, for which the expressions are recorded in Table 1. For the alkanols, values of the parameters practically coincide with those reported in previous papers.^{2,3} The densities of the pure compounds are recorded in Table S3 in the Supporting Information, which also gives the V_m^E of the binary mixtures and the values obtained at 298.15 and 318.15 K. For $[\text{bpy}][\text{BF}_4]$ the densities were lower than those shown in the literature by Mokhtarami et al.,¹² of, respectively, 1213.4 and $1199.8 \text{ kg} \cdot \text{m}^{-3}$ probably due to a slightly higher water content in the IL used by these authors compared to that recorded by us, see Table 1. The exponential of the densities gives us a mean value for the thermal expansion coefficients in the temperature interval considered, and the obtained values are in agreement with those reported in the literature.

Description of the Computational Method. All the molecular energies, geometries and frequencies have been calculated using the B3LYP method in conjunction with a 6-31++G** basis set using the Gaussian 03 program.²³ The presence of a minimum of energy was ensured by the lack of imaginary vibrational frequencies. The molecular structures of the ionic liquid species (ion pairs and independent cation and anion) were initially optimized in the gas phase. In order to describe solvent effects, polar environments have been simulated by the polarizable continuum model (PCM) with different dielectric polarity. Finally, molecular models of solvated ionic liquids including clusters with a discrete number (1–3) of solvent molecules have been calculated to simulate acidic and basic specific interactions with the solvent. Theoretical free energies have been predicted at the B3LYP/6-31++G** computational level including electronic energies, zero-point energies, enthalpy temperature corrections and absolute entropies at 298.15 K and 1 atm derived using the calculated vibrational frequencies and standard statistical thermodynamics relationships. The isotropic ^1H NMR nuclear shieldings were calculated at the B3LYP/6-31++G** level using the GIAO method.²³ The conversion to chemical shifts was done using the experimental–theoretical linear correlations for ^1H NMR chemical shifts previously reported.¹⁶

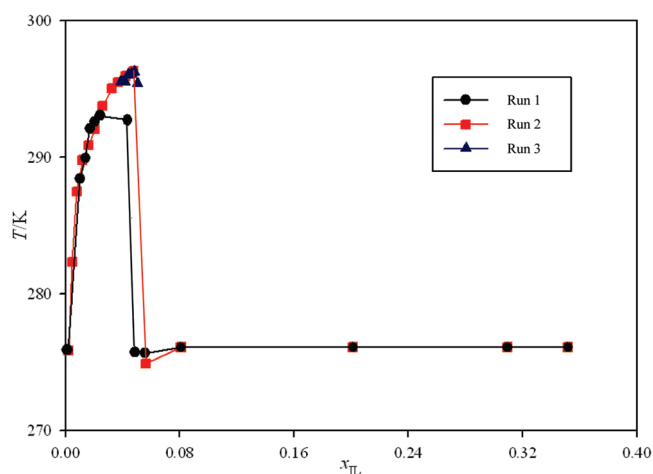
The standard procedure was applied for COSMO-RS calculations, which consists of two steps: First, Gaussian03 was used to compute the COSMO files. The ideal screening charges on the molecular surface for each species were calculated by the continuum solvation COSMO model using the BVP86/TZVP/DGA1 level of theory. Subsequently, COSMO files were used as an input in COSMOthermX²⁴ code to obtain the σ -profile and σ -potential of the pure compounds and to calculate the thermodynamic and thermochemical properties of binary water/alkanol–ionic liquid mixtures. The solubility intervals for binary mixtures were estimated by the COSMO-RS methodology using LLE_opt option and searching the phase diagram for the LLE point at different temperature. According to our chosen quantum method, the functional and the basis set, we used the corresponding parametrization (BP_TZVP_C21_0106).

RESULTS AND DISCUSSION

Liquid–Liquid Equilibria. The initial phase of the experimentation consisted of characterizing substances described in the above section and verifying the degree of miscibility of the

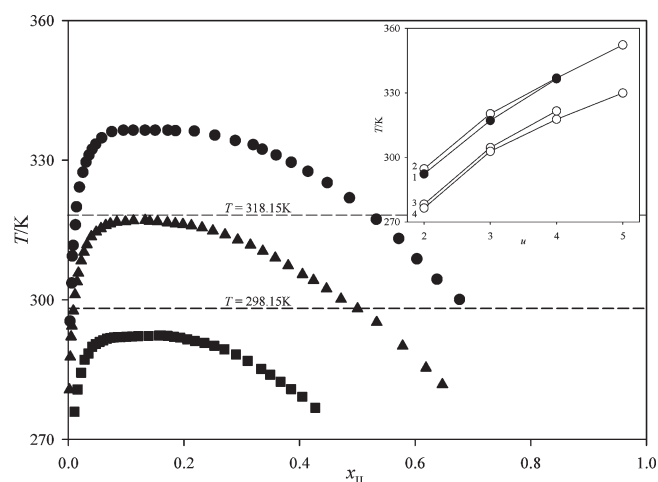
Table 1. Physical Properties of Pure Compounds: Purity %, w/w; Water Content by Karl Fischer Titration and Coefficients of Correlation of Density $\rho/(\text{kg} \cdot \text{m}^{-3})$, Refractive Index, n_D , and Viscosity, $\eta/(\text{mPa} \cdot \text{s})$, for the Temperature Range 288–328 K

compd	purity/%, w/w	water content, Karl Fischer/ppm, exptl	$\rho = A \exp(-\alpha T)$			$n_D = a + bT$		$\ln(\eta) = A + B/T$	
			A	$10^3(\alpha)$	$10^3(\alpha)$ lit.	a	$10^4(-b)$	A	B
[bpy][BF ₄]	>99.0	370	1437.1	0.57	0.57 ^a	1.5166	2	−14.0	5720.6
methanol	>99.8	40	1138.3	1.24	1.26 ^b	1.4465	4	−1.29	543.04
ethanol	>99.0	27	1104.9	1.14	1.15 ^b	1.4824	4	−3.57	1358.8
propan-1-ol	>99.0	57	1099.4	1.06	1.05 ^b	1.5015	4	−6.07	2293.6
butan-1-ol	>99.0	40	1088.9	1.01	1.00 ^b	1.5025	4	−11.5	4103.5
water			1102.4	0.34	0.34 ^b	1.3648	1		

^a Reference 12. ^b Reference 3.**Figure 2.** Representation of experimental $T-x_{\text{IL}}$ for the binary mixture [bpy][BF₄] + water indicating a short interval of miscibility.

mixtures selected, since it is important to define the composition intervals in each of these and the temperature zones corresponding to total miscibility, a space where the thermodynamic quantities of the mixing can be determined. Experience from previous studies with [bXmpy][BF₄] mixtures^{1–3} has shown that the ILs derived from pyridinium give rise to a certain ordering of the miscibility curves with the alkanols. However, the [bpy][BF₄] is not an isomer of the [bXmpy][BF₄], thus its phases may behave differently. Using the experimental cell already described in previous works,^{1,2} the miscibility curves of [bpy][BF₄] with water and the first four alkanols were determined.

Remarkably, [bpy][BF₄] shows a hydrophobic behavior in low-concentrated water solution in basis of the small immiscibility zone in the poorest region of IL ($x_{\text{IL}} < 0.05$) found in its mixtures with water (see Figure 2). This was confirmed by three different series of data, with a maximum difference of 3 °C between the first series and the other two, but at an upper critical solution temperature (UCST) very close between them, situated at the coordinates around 0.048 (Table S1 in the Supporting Information). This calculation was carried out by taking into account the amount of water in the IL determined by Karl Fischer, however the small influence of this correction in the final results has been checked. Regarding the alkanols, the solubility data are also shown in Table S1 in the Supporting Information. Figure 3 graphically represents the asymmetric zones that limit

**Figure 3.** Plots of experimental data $T-x_{\text{IL}}$ of the binary mixtures [bpy][BF₄] + ethanol (■), + propan-1-ol (▲), + butan-1-ol (●). Inset represents the variation of the upper critical solution temperature (UCST) as a function of the number of alkanol carbon atoms u in $\text{C}_u\text{H}_{2u+1}(\text{OH})$ for different ILs: 1, for binaries containing [bpy][BF₄], 2, 3, and 4 indicate the X-value in [bXmpy][BF₄].

the region of two LL phases and that of a single liquid phase. From the graph and the numerical data, the intervals that indicate zones of two phases at the temperatures chosen for this work are as follows: for the system [bpy][BF₄] + CH₃(CH₂)₂(OH) at 298.15 K, the interior ones at [0.011–0.473], mixture which becomes totally miscible in the whole interval [0,1] at 318.15 K. For the system [bpy][BF₄] + CH₃(CH₂)₃(OH), at 298.15 K, the two phase interval corresponds to the interior of [0.005–0.716], and at 318.15 K the interior of [0.013–0.524]. The binary systems with methanol and ethanol are completely miscible at the two working temperatures. The inset in Figure 3 shows the changes in UCST with alkanol chain length and the comparison with previously obtained values for mixtures of other pyridinium derivatives, [bXmpy][BF₄], published by our group previously.^{1–3} Differences are observed between the UCST values of the corresponding isomers at $X = 3$ and 4, whereas the isomer at $X = 2$ presents values close to those of [bpy][BF₄], which may be ascribed to the different degrees of packing that are also denoted by the similar densities of [bpy][BF₄] and [b2mpy][BF₄], respectively, 1213¹² and 1202³ kg·m^{−3} at 298.15 K, in contrast to the lower density values for [b3mpy][BF₄] and [b4mpy][BF₄] of, respectively, 1182¹ and 1183² kg·m^{−3} at 298.15 K.

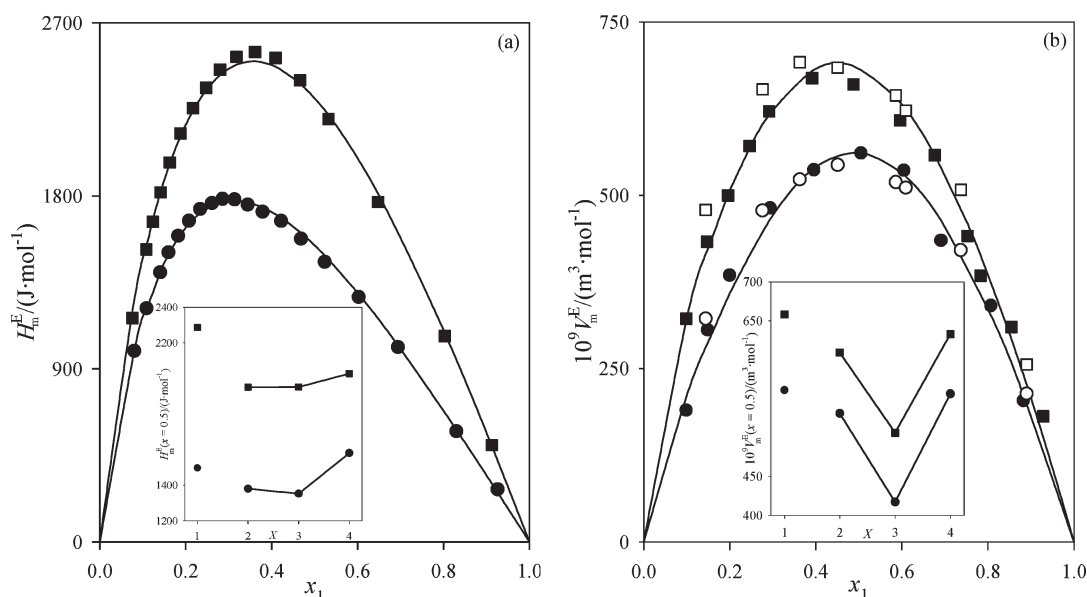


Figure 4. Experimental values obtained for the binary [bpy][BF₄] + water at 298.15 K (●) and at 318.15 K (■), and the corresponding fitting curves estimated by eq 1 for (a) H_m^E and (b) V_m^E . Open symbols are values reported by Mokhtarani et al.¹² at 298.15 K (○) and at 318.15 K (□). Insets represent the comparison between the H_m^E equimolar values (panel a) or V_m^E (panel b) for [bpy][BF₄] + water and those for [bXmpy][BF₄] + water, as a function of $X = 2, 3, 4$.

Excess Properties. Points corresponding to (x_{IL}, H_m^E) and (x_{IL}, V_m^E) for the mixtures studied at 298.15 and 318.15 K are presented for [bpy][BF₄] + water, or + alkanol, respectively, in Tables S2 and S3 in the Supporting Information. Sets of experimental data were correlated with a simple polynomial equation, where the excess property, represented generically by Y_m^E , H_m^E (in J·mol⁻¹) or $10^3 \cdot V_m^E$ (in m³·mol⁻¹), is expressed as a function of the so-called *active fraction*²⁵ $z_{IL}(x_{IL})$ of the [bpy][BF₄], by

$$Y_m^E = z_{IL}(1 - z_{IL}) \sum_{i=0}^2 y_i z_{IL}^i \quad \text{where} \quad (1)$$

$$z_{IL} = \frac{x_{IL}}{x_{IL} + k(T)(1 - x_{IL})}$$

with the coefficients y_i dependent on T as follows:

$$y_i = \sum_{j=0}^2 Y_{ij} T^{j-1} \quad (2)$$

substituting in each case the coefficients Y_{ij} for those corresponding to the correlations of enthalpies h_{ij} or excess volumes v_{ij} . In this way, a single correlation can be obtained of the properties as a function of temperature, which means that others can then be estimated by derivation. The data correlation now requires the fit of an excess property with two variables, $Y_m^E(x_{IL}, T)$, for which an algorithm for nonlinear functions has been employed.

In previous works,^{3,25} for correlation of the V_m^E it was proposed that parameter k could be determined as the quotient of molar volumes of pure compounds of the mixture in working conditions, p and T , which, considering a reference temperature of T_0 , adopts the form

$$\begin{aligned} k_v(T) &= \frac{V_i^0(T)}{V_{IL}^0(T)} = \frac{M_i}{M_{IL}} \frac{\rho_{IL}(T_0)}{\rho_i(T_0)} [e^{(\alpha_{IL} - \alpha_i)(T - T_0)}] \\ &= k_v(T_0) [e^{(\alpha_{IL} - \alpha_i)(T - T_0)}] \end{aligned} \quad (3)$$

where α_i and α_{IL} , respectively, correspond to the thermal expansion coefficients of the compound i and of the IL, which are shown in Table 1.

On the other hand, in the correlation of the pairs of (x_{IL}, H_m^E) the parameter k is given by k_h , and when it is represented as a function of temperature, it has an analogous form to eq 3 and can be written as

$$k_h(T) = k_h(T_0) [e^{(2/3)(\alpha_{IL} - \alpha_i)(T - T_0)}] \quad (4)$$

where

$$\begin{aligned} k_h(T_0) &= \frac{S_i^0}{S_{IL}^0} = \left(\frac{q_i}{q_{IL}} \right) \left(\frac{r_{IL}}{r_i} \right)^{2/3} \left[\frac{V_i^0(T_0)}{V_{IL}^0(T_0)} \right]^{2/3} \\ &= k_q \left[\frac{k_v(T_0)}{k_r} \right]^{2/3} \end{aligned} \quad (5)$$

In summary, eqs 3 and 4 suggest a similar mathematical formula to express the variations of parameters k_v and k_h , respectively, with temperature. Since this is not an objective of the present work, we opted to present these parameters with a single form where the constant $k_v(T_0)$ and $k_h(T_0)$, expressed above, are substituted by parameters, noted as $k_{v,0}$ and $k_{h,0}$, whose optimum values are determined in the correlation process of V_m^E or H_m^E , respectively.

Binary Mixtures IL + Water. Experimental thermodynamic properties are presented in Tables S2 and S3 in the Supporting Information, and the corresponding fitting coefficients using eq 1 are in Table S4 in the Supporting Information. Figures 4a and 4b show the data and curves of (x_{IL}, H_m^E) and (x_{IL}, V_m^E) , respectively, for the binary [bpy][BF₄] + water, at temperatures of 298.15 and 318.15 K. The mixing processes of IL with water are endothermic, increasing with temperature, so the corresponding thermal coefficient is positive $(dH_m^E/dT)_p > 0$. To the best of our knowledge, for this mixture, there are no previous H_m^E data in

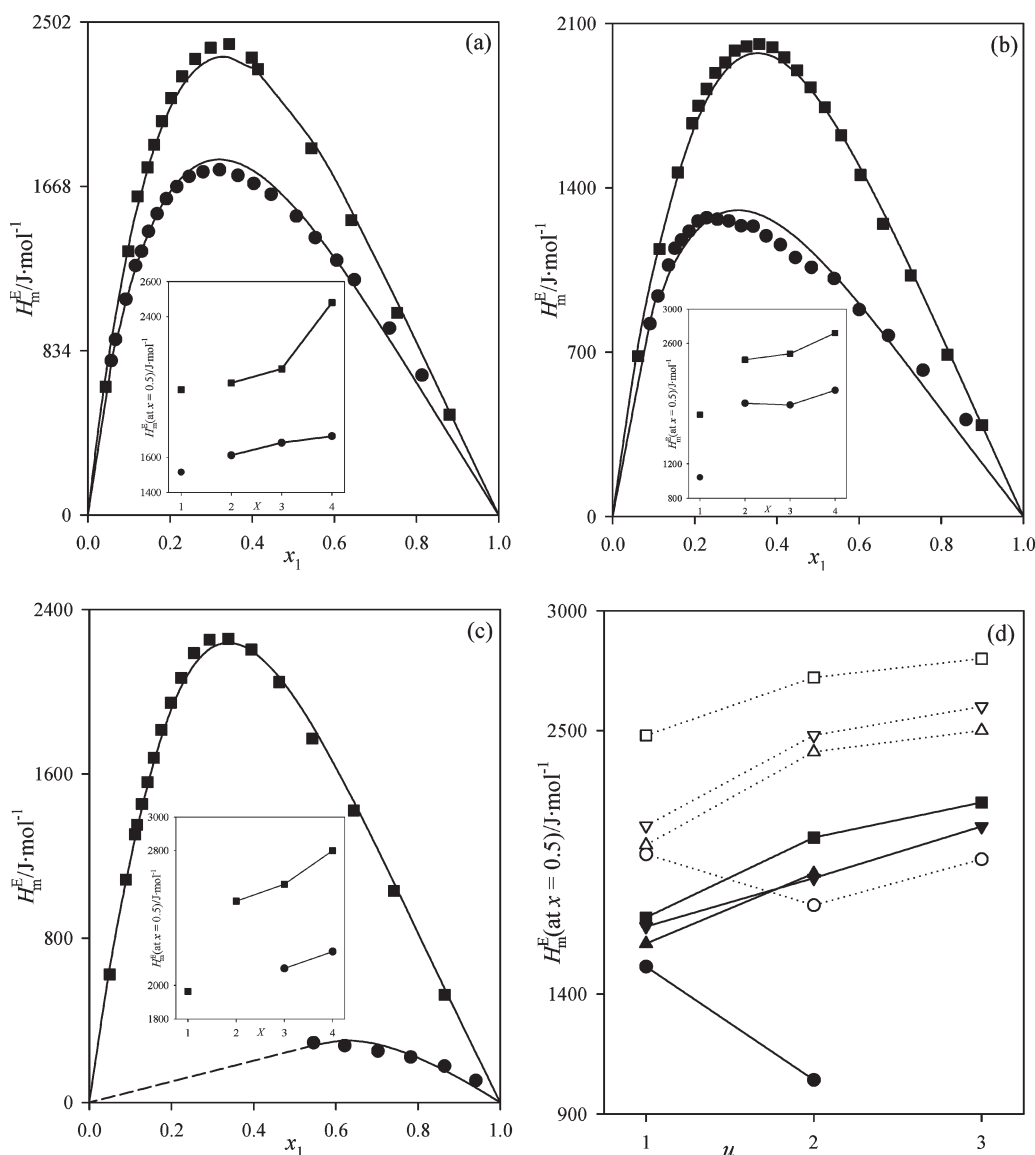


Figure 5. Experimental H_m^E values obtained for the binaries $[bpy][BF_4] + C_uH_{2u+1}(OH)$ at 298.15 K (●), and at 318.15 K (■), and the corresponding fitting curves estimated by eq 1. Insets represent the comparison between the equimolar values of this work and those from the literature^{1–3} for binaries $[bXmpy][BF_4]$ ($X = 2, 3, 4$) + $C_uH_{2u+1}(OH)$ $[bpy][BF_4]$ + water and those for $[bXmpy][BF_4]$ + water, as a function of $X = 2, 3, 4$. (a) for $u = 1$; (b) for $u = 2$; (c) for $u = 3$; (d) equimolar H_m^E values as a function of u for the binaries formed by $C_uH_{2u+1}(OH)$ and $[bpy][BF_4]$ (●, ○), $[b2mpy][BF_4]$ (▲, △), $[b3mpy][BF_4]$ (▼, ▽), $[b4mpy][BF_4]$ (■, □). Open symbols at 298.15 K and solid symbols at 318.15 K.

the literature. In the inset in Figure 4a, the changes in the equimolar values obtained in the aqueous mixtures of the isomers ($X = 2, 3$ and 4)^{1–3} and $[bpy][BF_4]$ are compared. As can be seen, the $[bpy][BF_4]$ + water mixture presents a generally stronger endothermic behavior than those for the series of butylmethylpyridines $[bXmpy][BF_4]$ previously reported by our group.^{1–3}

Figure 4b shows the values of $V_m^E(x_{IL})$ at the two working temperatures of the mixture $[bpy][BF_4]$ + water, together with data available in the literature¹² for V_m^E values at the same temperatures. The comparison with our data show slight differences at some points, but, in general, the agreement can be considered to be acceptable. The results of V_m^E show clear expansion effects that increase with temperature, and the coefficient $(dV_m^E/dT)_p$ is also positive

Binary Mixtures of IL + Alkanol. As shown in the corresponding section, the binary systems $[bpy][BF_4]$ + methanol, or + ethanol

were totally miscible in the entire range of compositions at the two working temperatures. However, mixtures with the other alkanols present immiscibility zones in which the properties cannot be measured, which are defined in Table S1 in the Supporting Information and Figure 3. Experimental values for these mixtures are in Tables S2 and S3 in the Supporting Information and the correlation coefficients in Table S4 in the Supporting Information.

Figures 5a–d and 6a–d show, respectively, the experimental data of H_m^E and V_m^E with the corresponding correlation curves obtained for all $[bpy][BF_4]$ + alkanol mixtures studied in this work, showing the interval of compositions that present immiscibility with a discontinuous line. The H_m^E are positive, see Figure 5a–d, for all these systems, with a likewise positive effect for temperature, in other words with $(dH_m^E/dT)_p > 0$. As can be seen in Figure 5d, the endothermicity of equimolar mixture at

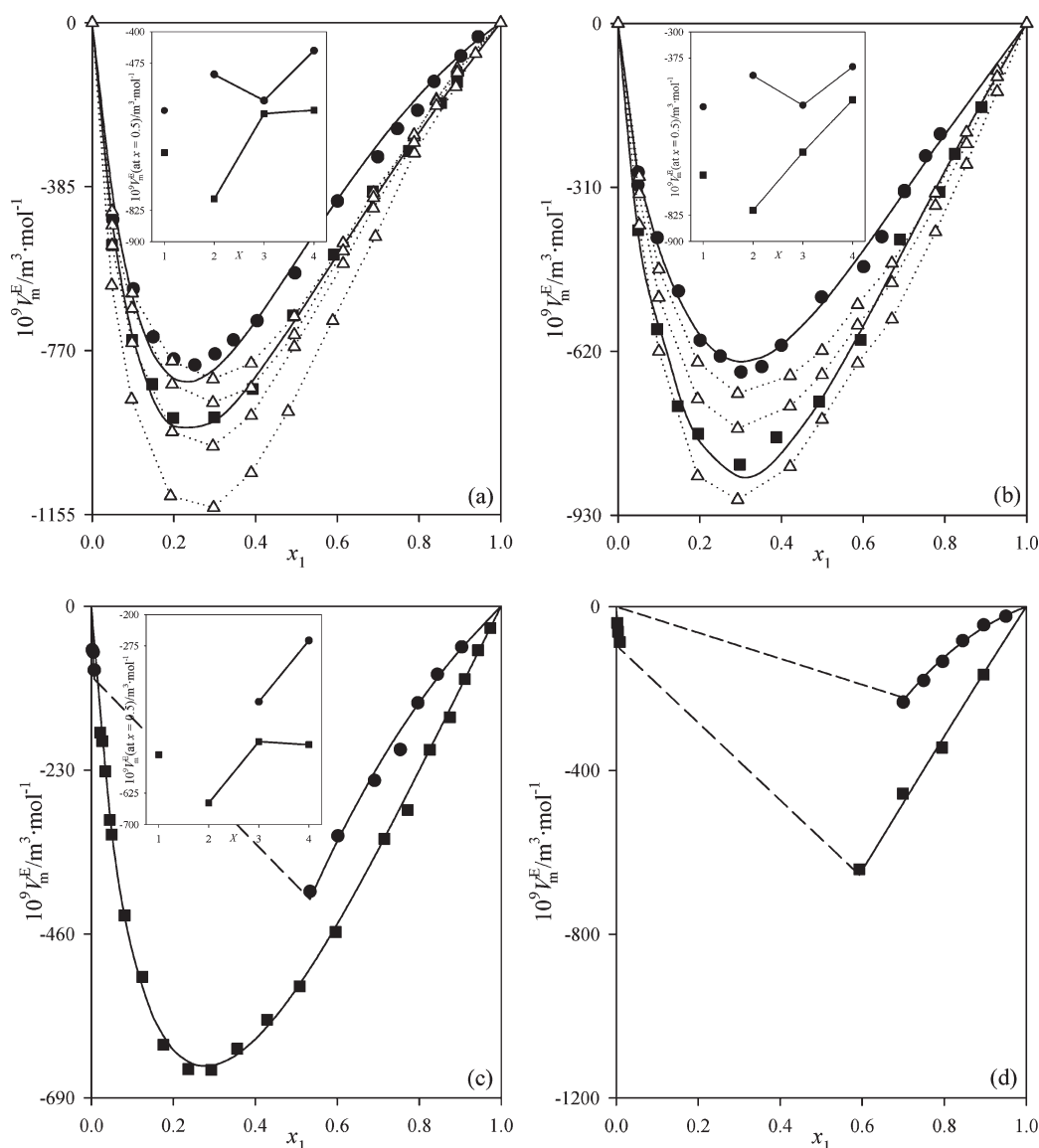


Figure 6. Experimental V_m^E values obtained for the binaries $[\text{bpy}][\text{BF}_4] + \text{C}_u\text{H}_{2u+1}(\text{OH})$ at 298.15 K (\bullet), and at 318.15 K (\blacksquare), and the corresponding fitting curves estimated by eq 1. Insets represent the comparison between the equimolar values of this work and those from literature^{1–3} for binaries $[\text{bXmpy}][\text{BF}_4]$ ($X = 2, 3, 4$) + $\text{C}_u\text{H}_{2u+1}(\text{OH})$. (a) for $u = 1$, comparison between our values and those from literature;¹³ (b) for $u = 2$, comparison between our values and those from literature;¹³ (c) for $u = 3$; (d) for $u = 4$.

298.15 K decreases with the chain length of alkanol (methanol > ethanol), while at 318.15 K an inversion occurs, with the endothermicity decreasing in the order methanol > ethanol, which is later followed by an increase for propan-1-ol. A comparison of the equimolar values in the insets with those obtained for the $[\text{bXmpy}][\text{BF}_4]$ in previous works^{1–3} indicated that the absence of the $-\text{CH}_3$ group from the molecule of $[\text{bpy}][\text{BF}_4]$ produces lower interaction energies, with differences increasing in the order methanol < ethanol < propan-1-ol, since the endothermicity $[\text{bXmpy}][\text{BF}_4] + \text{alkanol}$ mixtures always increases with the alkyl chain of the organic solvent.

In relation to V_m^E measurements, which are represented at two temperatures in Figures 6a–d, in all cases a clear contraction effect is noticed, which decreases as the alkanol chain length increases. By contrast, the contraction increases with temperature. Figures 6a,b also show the V_m^E of the systems $[\text{bpy}][\text{BF}_4] + \text{methanol}$, or + ethanol published by García-Mardones et al.¹³ for

purposes of comparison, although these were obtained at temperatures (293.15, 303.15, 313.15, and 323.15 K) different from those used in this work. Our data are in good agreement with those previously reported for $[\text{bpy}][\text{BF}_4] + \text{ethanol}$, although there are slight differences in the curves corresponding to the $[\text{bpy}][\text{BF}_4] + \text{methanol}$ system, which are not easily explained. The greatest differences are observed in the inflections in the curves, owing to the different sizes of the participating molecules. These are most extreme for the case of methanol, as it was reported by the authors mentioned above.¹³

The insets in Figures 6a–c show comparisons of the equimolar values of V_m^E in this work for $[\text{bpy}][\text{BF}_4] + \text{alkanol}$ mixtures to those recorded for isomers $[\text{bXmpy}][\text{BF}_4]$ ($X = 2, 3, 4$) + alkanol mixtures in previous works.^{1–3} Although some anomalies are observed in the distribution, the contractions are lower in mixtures with $[\text{bpy}][\text{BF}_4]$ at both temperatures, with the exception of methanol and ethanol at the temperature of 318.15 K, for

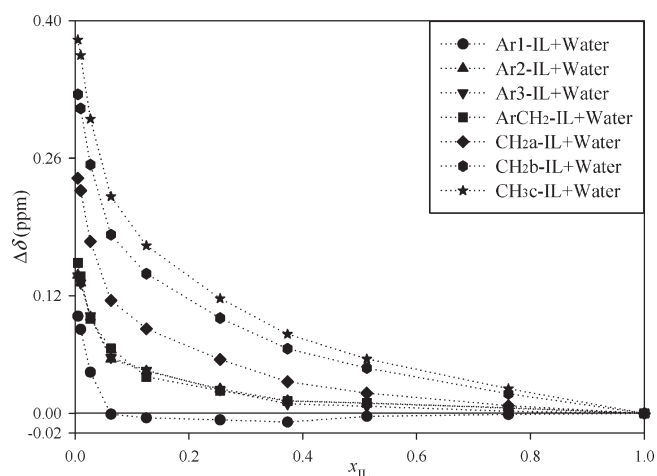


Figure 7. Change in chemical shift of $[\text{bpy}][\text{BF}_4]$ protons in mixtures with water relative to their chemical shift in pure IL as a function of the molar fraction of $[\text{bpy}][\text{BF}_4]$. Hydrogen atom classification: Ar1-IL (●), Ar2-IL (▲), Ar3-IL (▼), ArCH₂-IL (■), CH_{2a}-IL (◆), CH_{2b}-IL (●) and CH₃-IL (★).

which they decrease with the IL of $X = 2$. These effects show that the presence of the $-\text{CH}_3$ group increases the steric impediment of the mixture, slightly reducing the contraction in the final mixture. In summary, with the results obtained and observations made about the properties, we have complemented the analysis performed for these mixtures in our previous works^{1–3} and, also, in the works of other authors.^{12,13}

¹H NMR Spectroscopy. A series of ¹H NMR spectroscopy experiments were conducted to try to explain the effects of the intermolecular interactions on the results of mixing properties of $[\text{bpy}][\text{BF}_4]$ + water or $[\text{bpy}][\text{BF}_4]$ + alkanol. Interactions such as the formation of hydrogen bonds between the different species present in a mixture (cation, anion or solvent) or a change in their electronic environment leads to changes in the chemical displacement of the protons involved. The magnitude of this change and its relationship with the composition provide information about what is happening at a molecular level.

Hence, in Figure 7 appear the relative displacements, $\Delta\delta$, of the cation protons in relation to the molar fraction of the IL, x_{IL} , for the mixture $[\text{bpy}][\text{BF}_4]$ + H₂O. These $\Delta\delta$'s are defined by the difference of the displacements of the same proton in the mixture with respect to the pure IL compound. Figure 8 represents the $\Delta\delta$ of selected protons (one aromatic and one aliphatic) for three different solvents: water, methanol and ethanol. Owing to the immiscibility of the other alkanols, propan-1-ol and butan-1-ol, at the experimental temperature of 293 K, they could not be included in this series. In all cases, we observe a gradual increase in $\Delta\delta$ with the addition of solvent to the pure IL (as x_{IL} decreases). This increase reflects stronger solvent effects by the formation of hydrogen bonds between the protons of pyridinic group and the solvent. Displacements of the aromatic protons were also found to be smaller than those of aliphatic protons. These displacements for aromatic and aliphatic hydrogens are clearly greater in alkanol mixtures than in water mixtures, the $\Delta\delta$ of $[\text{bpy}][\text{BF}_4]$ + methanol being similar to those of $[\text{bpy}][\text{BF}_4]$ + ethanol.

Similarly, the $\Delta\delta$ values of the protons of the solvent decrease with increasing concentration of the IL, see Figure 9. This was only to be expected, like the formation of hydrogen bonds with

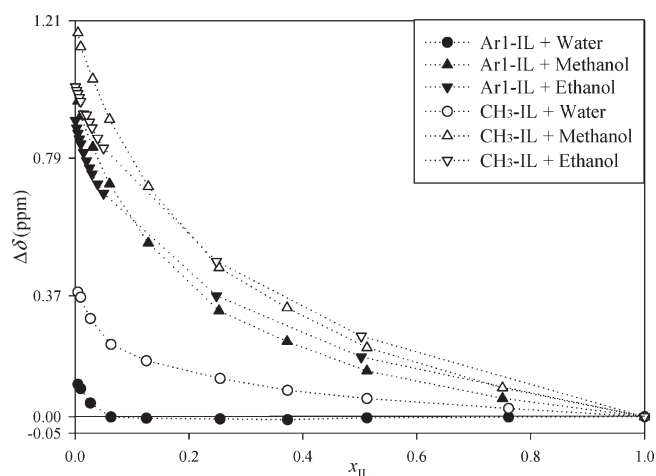


Figure 8. Change in chemical shift of two/selected $[\text{bpy}][\text{BF}_4]$ protons in mixtures with water or alkanol relative to their chemical shift in pure IL as a function of the molar fraction of $[\text{bpy}][\text{BF}_4]$. Hydrogen atom classification: Ar1-IL + water (●), CH₃-IL + water (○); Ar1-IL + methanol (▲), CH₃-IL + methanol (Δ); Ar1-IL + ethanol (▼), CH₃-IL + ethanol (▽).

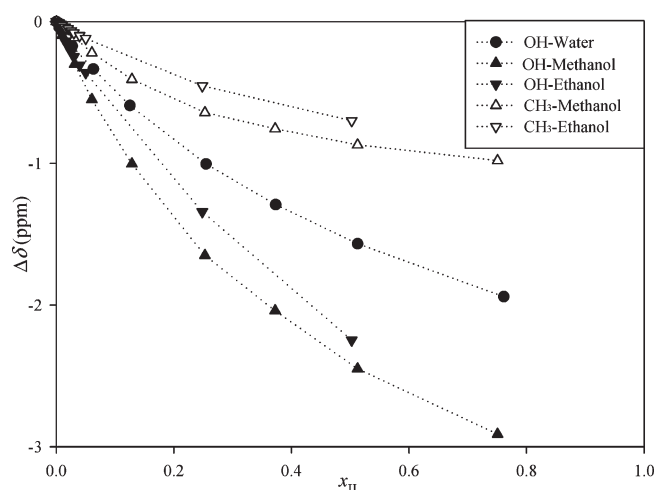


Figure 9. Change in chemical shift of selected alkanol protons in mixtures of $[\text{bpy}][\text{BF}_4]$ with water, methanol and ethanol relative to their chemical shift in pure alkanol as a function of the molar fraction of $[\text{bpy}][\text{BF}_4]$; OH-water + IL (●); OH-methanol + IL (▲); OH-ethanol + IL (▼), CH₃-methanol + IL (Δ); CH₃-ethanol + IL (▽).

the IL—especially with the anion—reflecting less self-association (effects of hydrogen bonds in identical molecules), and clearly, as the latter are stronger than the former, there is a decrease in the $\Delta\delta$. The effect is greater for protons of the hydroxyl group, which are directly involved in the hydrogen bonds.

At least theoretically, it is possible that the intermolecular interactions cause the formation of solvent–IL aggregates²⁶ and micelles,²⁷ in which apolar zones can be distinguished, composed of alkyl chains, and polar zones, composed of the pyridinic ring and the anions, which has recently indicated of pyridinium based ILs.²⁸ To determine whether this is present in the systems studied, in this work we have plotted the graphs for $\Delta\delta$ as a function of the reciprocal concentration, Figure S1 in the Supporting Information. In all cases, a gradual/reciprocal change

is observed in $\Delta\delta$ with the change in composition of the IL, both for the protons of the IL and for those of the solvent. The absence of discontinuities or brusque changes in the slopes of the curves seems to indicate that there is no critical aggregation concentration. Finally, we did not observe any particular behavior for $[\text{bpy}][\text{BF}_4]$ + alkanol mixtures that could explain the different behavior of H_m^E with alcohol chain size with respect to that found for the $[\text{bXmpy}][\text{BF}_4]$ series. In fact, the mixtures of $[\text{b2mpy}][\text{BF}_4]$ show very similar $\Delta\delta$ dependences on concentration to those observed for $[\text{bpy}][\text{BF}_4]$ + ROH, for water, methanol and ethanol, and the order is the same with similar or greater $\Delta\delta$'s for $[\text{bpy}][\text{BF}_4]$ for all the protons (this tendency is shown in Figure S2 in the Supporting Information for equimolar values).

■ QUANTUM CHEMICAL ANALYSIS

Following, we develop a computational analysis based on quantum-chemical methods to obtain some insights about the intermolecular interactions between $[\text{bpy}][\text{BF}_4]$ and water or alkanol compounds, which could determine their mixture behavior. The above ^1H NMR results showed significant effects on the chemical shift signals of $[\text{bpy}][\text{BF}_4]$ and water or alkanol compounds by mixing, which were assigned to IL–solvent interactions, mainly hydrogen bonding, as it was demonstrated for imidazolium based ILs.¹⁶ In addition, FT-IR spectroscopy studies have also supported that the hydrogen bonds play an

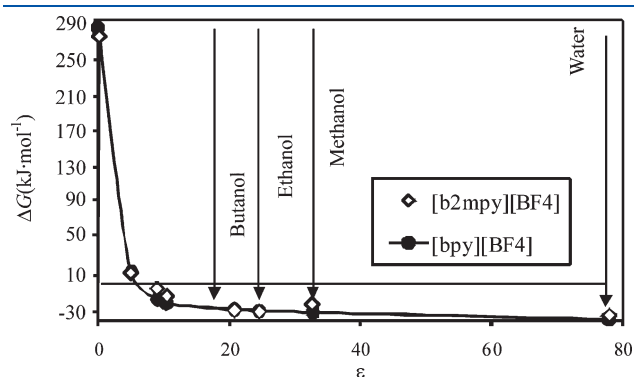


Figure 10. Dissociation free energies ($\text{CA} \rightarrow \text{C}^+ + \text{A}^-$) for the ILs $[\text{bpy}][\text{BF}_4]$ and $[\text{b2mpy}][\text{BF}_4]$, calculated at the PCM-B3LYP/6-31++G** level as a function of solvent dielectric constant ϵ at 298.15 K.

important role in interactions between ILs and solvents,¹⁴ hydrogen bonding between $[\text{bpy}][\text{BF}_4]$ and water molecules being recently described.¹⁵ Hence, it has been shown that the addition of water to pure $[\text{bpy}][\text{BF}_4]$ gradually destroys the tridimensional structure of the IL, first composed of ion pairs surrounded by molecules of solvent and, finally, generating independent ions completely solvated by water.¹⁵ However, other studies carried out on ILs based on the imidazolium cation show that complete dissociation of the ion pairs only takes place when the molar concentration of the IL is extremely low, while, as this increases, clusters of the IL begin to form that interact with molecules of the solvent.¹⁴ Consequently, there is some controversy in the current literature about the most appropriate molecular model to simulate adequately the behavior of the IL compound in a mixture.^{29,30} In order to study the possible presence of different species of IL in the study mixtures, we first estimated the dissociation Gibbs energy of the ion pair in its independent ions ($\text{CA} \rightarrow \text{C}^+ + \text{A}^-$) for the ILs $[\text{bpy}][\text{BF}_4]$ and $[\text{b2mpy}][\text{BF}_4]$ at 298.15 K as a function of the dielectric constant of the solvent, using the quantum chemistry model PCM-B3LYP/6-31++G** described previously,¹⁶ for which the computational procedure is shown in detail in the Experimental Section. As can be observed in Figure 10, the calculations indicate that both ILs are completely dissociated in the mixture with all the solvents studied, in accordance with experimental evidence.¹⁵ This suggests that a molecular model of independent ions ($\text{C}^+ + \text{A}^-$) may be more appropriate to simulate the mixtures $[\text{bpy}][\text{BF}_4]$ or $[\text{b2mpy}][\text{BF}_4]$ + water/alkanol than that of the ion pairs (CA). Continuing with analysis of the appropriate molecular model to describe the mixing properties of $[\text{bpy}][\text{BF}_4]$, the GIAO-B3LYP/6-31++G** estimation was made with the chemical displacements (^1H NMR) of the signals of $[\text{bpy}][\text{BF}_4]$ as a function of the solvent, using the CA ion-pair model, Figure 11a, and the independent ions $\text{C}^+ + \text{A}^-$, Figure 11b. As can be observed, the quantum-chemistry observations ^1H NMR of $[\text{bpy}][\text{BF}_4]$ obtained by an ion-pair molecular model (CA) are not in close agreement with experimental evidence, Figure 11a, since the calculations predict a smaller displacement from the AR1-IL signal of the $[\text{bpy}][\text{BF}_4]$ in the solvent, in contrast with experimental results. On the contrary, identical calculations of chemical displacements ^1H NMR of $[\text{bpy}][\text{BF}_4]$ using a molecular model of independent ions ($\text{C}^+ + \text{A}^-$) significantly improve the results, although there is no clear agreement between

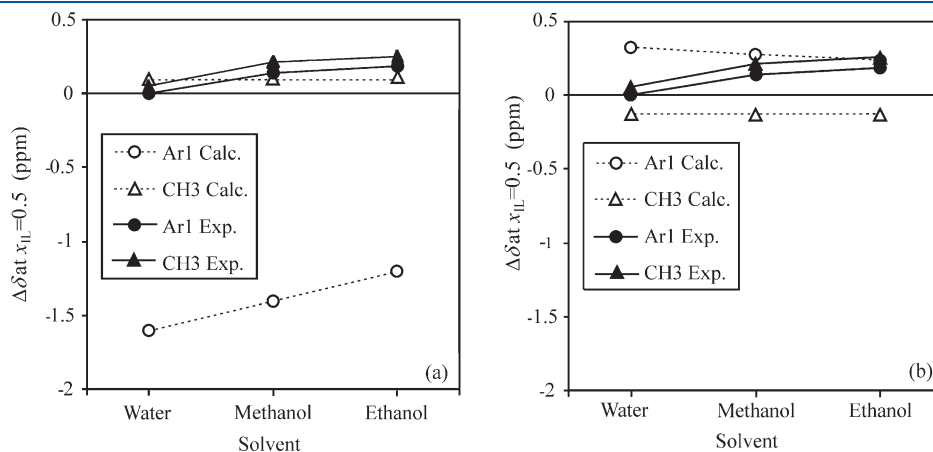


Figure 11. Estimation GIAO-B3LYP/6-31++G** of the chemical displacements (^1H NMR) of $[\text{bpy}][\text{BF}_4]$ as a function of solvent using the ion-pair molecular model CA (a) and the independent ion molecular model $\text{C}^+ + \text{A}^-$ (b).

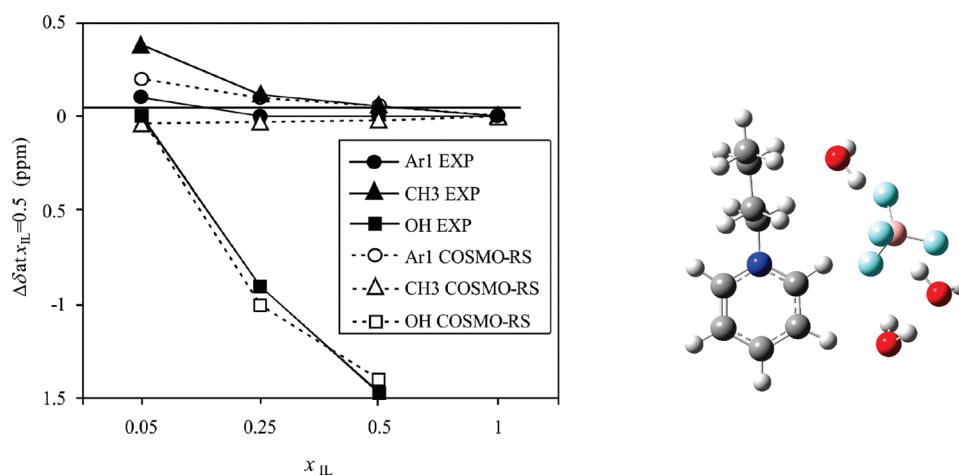


Figure 12. Example of the molecular model $[\text{bpy}][\text{BF}_4] \cdot n\text{H}_2\text{O}$ to simulate the presence of associated species IL–solvent and estimation GIAO-B3LYP/6-31++G** of the chemical displacements (^1H NMR), as a function of the mixing composition obtained by a molecular model $[\text{bpy}][\text{BF}_4] \cdot n\text{H}_2\text{O}$.

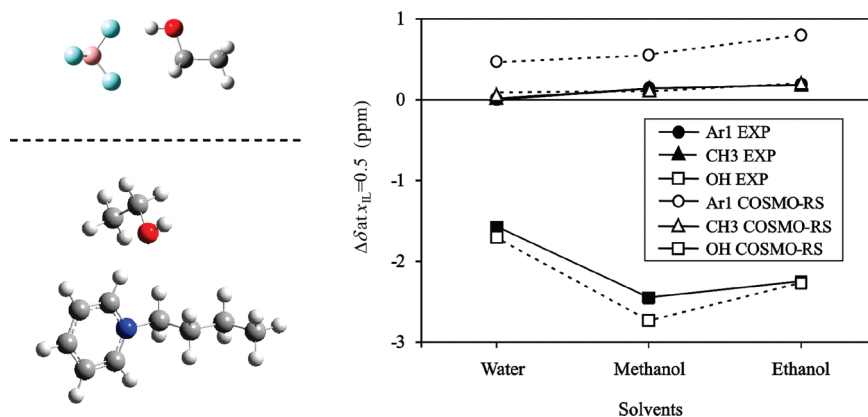


Figure 13. Estimation GIAO-B3LYP/6-31++G** of the chemical displacements (^1H NMR) of $[\text{bpy}][\text{BF}_4]$ as a function of solvent obtained by the ion–solvent molecular models: $[\text{bpy}]^+ \cdot 1$ solvent or $[\text{BF}_4]^- \cdot 1$ solvent.

theoretical and experimental data for the tendencies of the ^1H NMR signals as a function of the solvent of the mixture. As it was noted, there is spectroscopic evidence for the presence of hydrogen bonding local interactions between the ionic liquid and the water molecules, which simultaneously act as donor and acceptor of hydrogen bonds, associated species of IL–solvent appearing in solution.¹⁵ Based on this, theoretical estimations of NMR signals of the $[\text{bpy}][\text{BF}_4]$ + water/alkanol mixtures were tested using molecular models including clusters of cation + anion + solvent (such as the model $[\text{bpy}][\text{BF}_4] \cdot 3\text{H}_2\text{O}$ shown in Figure 12). The first significant result was that the water molecules are located between the cation and the anion, increasing the distance between them. Consequently, strong hydrogen bonds are formed between the C–H groups of the pyridinic ring and the oxygen of the water, increasing the chemical displacement of the Ar-1 ^1H NMR signal of pyridine with the composition of water molecules in the mixture, Figure 12. Similarly, interactions are observed between the hydrogens of the alkyl chain of the cation and the oxygen group of the water, resulting in increased ^1H NMR signals. On the other hand, the anion $[\text{BF}_4]^-$ forms hydrogen bonds with the water molecules, although these interactions are weaker than those formed by the

water molecules, so the ^1H NMR signals of the water decrease with the molar fraction of the IL in the mixture. On the basis of the promising theoretical results obtained using clusters that include molecules of solvent, the next step was to consider the total dissociation of the IL in solution. Hence, calculations of the ^1H NMR signals of the mixtures were made using associated species of cation $\cdot 1$ solvent molecule and anion $\cdot 1$ solvent molecule, as shown in Figure 13. The quantum-chemistry estimations of the chemical displacements show an excellent agreement with experimental data, and, therefore, current results indicated the presence of associated species of ion–solvent by local hydrogen-bond-type interactions in the mixtures of IL + water or alkanols.

Based on this computational analysis, the choice of molecular model used to simulate the IL in methods as COSMO-RS or UNIFAC should be determinant for the accuracy of thermodynamic data predictions. As an example, Figure 14 shows the different COSMO-RS predictions of the solubility values for the mixtures $[\text{bpy}][\text{BF}_4]$ + water/alkanol by applying an ion pair model (CA) or independent ion ($\text{C}^+ + \text{A}^-$). As it is shown in Figure 14a, the experimental solubility of $[\text{bpy}][\text{BF}_4]$, with its small hydrophobicity at low IL concentration, presents values

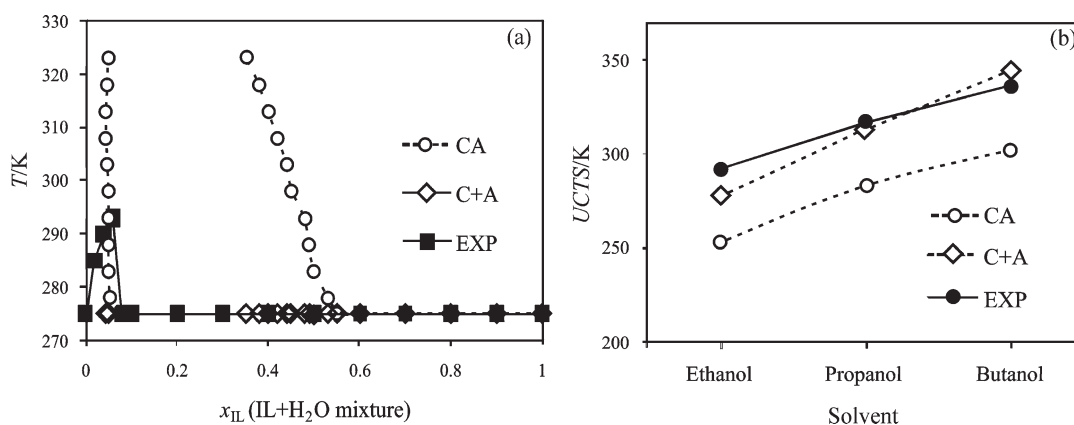


Figure 14. Predictions by COSMO-RS of liquid–liquid equilibria for mixtures: (a) [bpy][BF₄] + water and (b) [bpy][BF₄] + alkanol, using the ion-pair molecular model (CA) and the independent ion molecular model (C⁺ + A[−]).

intermediate between those predicted by the above simple CA and C⁺ + A[−] models. Thus, the neutral ion pair model (CA) predicted a high hydrophobicity of the IL by COSMO-RS while the independent ion model (C⁺ + A[−]) predicts complete miscibility in water. On the other hand, the COSMO-RS calculated data for the upper critical solution temperature (UCST) of mixtures [bpy][BF₄] + alkanol mixtures (Figure 14b) were clearly better using the independent ion model C + A, providing trends in reasonable agreement with experimental data. On the other hand, in previous studies,^{3,4} the ion-pair model (CA) gave rise to reasonable excess enthalpies of [bXmpy][BF₄] mixtures with different solvents. In summary, current calculations revealed the importance of the structural model used to simulate the mixtures of pyridinium-based ILs with water or alkanol in the methods of predicting thermodynamic data and COSMO-RS or UNIFAC, which will be analyzed with detail in further studies by our group.

CONCLUSIONS

Knowledge of the influence of different factors on solution behavior of ionic liquids with other solvents is useful for using ILs in specific applications. In this work the authors have measured several pure (density, refractive index and viscosity) and mixing (solubility, excess enthalpy and excess volume) properties of [bpy][BF₄] + water and alkanol mixtures, including a NMR spectroscopic study, in order to clarify the behavior of pyridinium-based ILs with several common solvents, comparing the results obtained here, using [bpy][BF₄], with those using [bXmpy][BF₄] (X = 2, 3, 4), previously obtained by our group.^{1–3} In reference to the mutual solubility of [bpy][BF₄], a slight hydrophobicity was observed, and that an increase in the alkyl chain length of the alkanols results in a regular increase in the UCST, since it becomes more aliphatic and less able to interact with the [bpy][BF₄] through hydrogen bonds and electrostatic forces. The measurements of excess properties showed that, in the mixtures [bpy][BF₄] + water, the $H_m^E > 0$ and $V_m^E > 0$ both increase with T , while the [bpy][BF₄] + alkanols give rise to $H_m^E > 0$ and $V_m^E < 0$. Similar mixing behavior by H_m^E and V_m^E data was found in previous works^{1–3} for [bXmpy][BF₄] + water mixtures, while for [bpy][BF₄] + alkanol mixtures a decreasing the endothermicity with the alcohol size was observed, in contrast with the results previously obtained for the [bXmpy][BF₄] series. NMR and quantum-chemical studies were performed to analyze the influence of IL–solvent interactions in the mixing properties

of [bpy][BF₄]/[bXmpy][BF₄] + water/alkanol mixtures. Results indicated the need of considering local hydrogen bonding interactions to analyze the behavior of these mixtures. As a consequence, the selection of the molecular model is a fundamental aspect to be considered for the adequate prediction of the thermodynamic properties of [bpy][BF₄]/[bXmpy][BF₄] + water/alkanol mixtures by widely used methods such as COSMO-RS and UNIFAC. This will be explored in greater depth in future studies by our research team.

ASSOCIATED CONTENT

S Supporting Information. Tables containing the experimental values of solubilities (S1), excess molar enthalpies (S2), excess molar volumes (S3) and correlation coefficients (S4). This material is available free of charge via the Internet at <http://pubs.acs.org>.

AUTHOR INFORMATION

Corresponding Author

*E-mail: jortega@dip.ulpgc.es.

Present Addresses

[†]Sección de Ingeniería Química (Dpto. de Química-Física Aplicada), Universidad Autónoma de Madrid, Cantoblanco, 28049 Madrid, Spain

ACKNOWLEDGMENT

The authors gratefully acknowledge the financial support received from Ministerio de Ciencia e Innovación (Spain) for Projects CTQ2009-12482 and CTQ2008-05641. We are very grateful to “Centro de Computación Científica de la Universidad Autónoma de Madrid” for computational facilities.

REFERENCES

- (1) Ortega, J.; Vreekamp, R.; Marrero, E.; Penco, E. Thermodynamic properties of 1-butyl-3-methylpyridinium tetrafluoroborate and its mixtures with water and alkanols. *J. Chem. Eng. Data* **2007**, *52*, 2269–2276.
- (2) Ortega, J.; Vreekamp, R.; Penco, E.; Marrero, E. Mixing thermodynamic properties of 1-butyl-4-methylpyridinium tetrafluoroborate [b4mpy][BF₄] with water and with an alkan-1-ol (methanol to pentanol). *J. Chem. Thermodyn.* **2008**, *40*, 1087–1094.

- (3) Navas, A.; Ortega, J.; Vreekamp, R.; Marrero, E.; Palomar, J. Experimental Thermodynamic Properties of 1-Butyl-2-Methylpyridinium Tetrafluoroborate [b2mpy] [BF₄] with Water and with Alkan-1-ol and their Interpretation with the COSMO-RS Methodology. *Ind. Eng. Chem. Res.* **2009**, *48*, 2678–2690.
- (4) Navas, A.; Ortega, J.; Palomar, J.; Diaz, C.; Vreekamp, R. COSMO-RS analysis on mixing properties obtained for the systems 1-butyl-X-methylpyridinium tetrafluoroborate [X = 2,3,4] and 1, ω -dibromoalkanes [ω =1–6]. *Phys. Chem. Chem. Phys.* **2011**, *13*, 7751–7759.
- (5) Law, M. C.; Cheung, T. W.; Wong, K.-Y.; Chan, T. H. Synthetic and Mechanistic Studies of Indium-Mediated Allylation of Imines in Ionic Liquids. *J. Org. Chem.* **2007**, *72*, 923–929.
- (6) Zhao, W.; Mo, Y.; Pu, J.; Bai, M. Effect of cation on micro-nano tribological properties of ultra-thin ionic liquid film. *Tribol. Int.* **2009**, *42*, 828–835.
- (7) Noda, A.; Watanabe, M. Highly conductive polymer electrolytes prepared by in situ polymerization of vinyl monomers in room temperature molten salts. *Electrochim. Acta* **2000**, *45*, 1265–1270.
- (8) Holbrey, J. D.; López-Martín, I.; Rothenberg, G.; Seddon, K. R.; Silvero, G. Desulfurisation of oils using ionic liquids: selection of cationic and anionic components to enhance extraction efficiency. *Green Chem.* **2008**, *10*, 87–92.
- (9) Ficke, L. E.; Novak, R. R.; Brennecke, J. F. Thermodynamic and Thermophysical Properties of Ionic Liquid + Water Systems. *J. Chem. Eng. Data* **2010**, *55*, 4946–4950.
- (10) Ficke, L. E.; Brennecke, J. F. Interactions of Ionic Liquids and Water. *J. Phys. Chem. B* **2010**, *114*, 10496–10501.
- (11) Porcedda, S.; Marongiu, B.; Schirru, M.; Falconieri, D.; Piras, A. Excess enthalpy and excess volume for binary systems of two ionic liquids + water. *J. Therm. Anal. Calorim.* **2011**, *103* (1), 29–33.
- (12) Mokhtarani, B.; Sharifi, A.; Mortaheb, H. R.; Mirzaei, M.; Mafi, M.; Sadeghian, F. Density and viscosity of pyridinium-based ionic liquids and their binary mixtures with water at several temperatures. *J. Chem. Thermodyn.* **2009**, *41*, 323–329.
- (13) García-Mardones, M.; Perez-Gregorio, H.; Guerrero, V.; Bandrés, I.; Lafuente, C. Thermodynamic study of binary mixtures containing 1-butylpyridinium tetrafluoroborate and methanol or ethanol. *J. Chem. Thermodyn.* **2010**, *42*, 1500–1505.
- (14) Katayanagi, H.; Nishikawa, K.; Shimosaki, H.; Miki, K.; Westh, P.; Koga, Y. Mixing schemes in ionic liquid-H₂O systems: A thermodynamic study. *J. Phys. Chem. B* **2004**, *108*, 19451–19457.
- (15) Wang, N.; Zhang, q.; Wu, F.; Yu, Z. Hydrogen Bonding Interactions between a Representative Pyridinium-Based Ionic Liquid [BuPy][BF₄] and Water/Dimethyl Sulfoxide. *J. Phys. Chem. B* **2010**, *114*, 8689–8700.
- (16) Palomar, J.; Ferro, V. R.; Gilarranz, M. A.; Rodriguez, J. J. A Computational Approach to Nuclear Magnetic Resonance in 1-Alkyl-3-Methylimidazolium Ionic Liquids. *J. Phys. Chem. B* **2007**, *111*, 168–180.
- (17) Ortega, J.; Marrero, E.; Palomar, J. Description of Thermodynamic Behaviour of the Systems Formed by Alkyl Ethanoates with 1-Chloroalkanes Using the COSMO-RS Methodology Contributing with New Experimental Information. *Ind. Chem. Eng. Res.* **2008**, *3*, 475–479.
- (18) Gmehling, J.; Li, J.; Schiller, M. A. modified UNIFAC model. 2. Present parameter matrix and results for different thermodynamic properties. *Ind. Eng. Chem. Res.* **1993**, *32*, 178–193.
- (19) Kato, R.; Gmehling, J. Systems with ionic liquids: Measurement of VLE and gamma(infinity) data and prediction of their thermodynamic behavior using original UNIFAC, mod. UNIFAC(Do) and COSMO-RS(O1). *J. Chem. Thermodyn.* **2005**, *37*, 603–619.
- (20) Klamt, A. COSMO-RS: From Quantum Chemistry to Fluid Phase Thermodynamics and Drug Design; Elsevier: Amsterdam, 2005.
- (21) Stokes, R. H.; Marsh, K. N.; Tomlins, R. P. An isothermal displacement calorimeter for endothermic enthalpies of mixing. *J. Chem. Thermodyn.* **1969**, *1*, 211–221.
- (22) Van Ness, H. C.; Abbott, M. M. *Int. DATA Ser., Sel. Data Mixtures, Ser. A* **1976**, *1*, 22.
- (23) Frisch, M. J.; et al. GAUSSIAN 03, Revision C.02; Gaussian, Inc.: Wallingford, CT, 2004.
- (24) Eckert, F.; Klamt, A. COSMOtherm, Version C2.1, Release 01.06; COSMOlogic GmbH & Co. KG: Leverkusen, Germany, 2006.
- (25) Ortega, J.; Espiau, F.; Vreekamp, R.; Tojo, J. Modelling and Experimental Evaluation of Thermodynamic Properties for Binary Mixtures of Dialkylcarbonate and Alkanes Using a Parametric Model. *Ind. Chem. Eng. Res.* **2007**, *46*, 7353–7366.
- (26) Dorbritz, S.; Ruth, W.; Kragl, U. Investigation on Aggregate Formation of Ionic Liquids. *Adv. Synth. Catal.* **2005**, *347*, 1273–1279.
- (27) Bowers, J.; Butts, C. P.; Martin, P. J.; Vergara-Gutierrez, M. C.; Heenan, R. K. Aggregation behavior of aqueous solutions of ionic liquids. *Langmuir* **2004**, *20*, 2191–2198.
- (28) Kodama, K.; Tsuda, R.; Niitsuma, K.; Tamura, T.; Ueki, T.; Kokubo, H.; Watanabe, M. Structural effects of polyethers and ionic liquids in their binary mixtures on lower critical solution temperature liquid-liquid phase separation. *Polym. J.* **2011**, *43*, 242–248.
- (29) Singh, T.; Kumar, A. Aggregation Behaviour of Ionic Liquids in Aqueous Solutions: Effect of Alkyl Chain Length, Cations and Anions. *J. Phys. Chem. B* **2007**, *111*, 7843–7851.
- (30) Diedenhofen, M.; Klamt, A. COSMO-RS as a tool for property prediction of IL mixtures-A review. *Fluid Phase Equilib.* **2010**, *294*, 31–38.